



Published in final edited form as:

*Arch Oral Biol.* 2015 May ; 60(5): 690–697. doi:10.1016/j.archoralbio.2015.02.020.

## Radiotherapy Effect on Nano-mechanical Properties and Chemical Composition of Enamel and Dentin

R. Reed<sup>a</sup>, C. Xu<sup>a</sup>, Y. Liu<sup>a</sup>, J.P. Gorski<sup>a,b</sup>, Y. Wang<sup>a,b</sup>, and M.P. Walker<sup>a,b</sup>

<sup>a</sup>Department of Oral and Craniofacial Sciences, School of Dentistry, University of Missouri-Kansas City, MO

<sup>b</sup>Center of Excellence in Musculoskeletal and Dental Tissues, University of Missouri-Kansas City, MO

### Abstract

**Objective**—To understand radiotherapy-induced dental lesions characterized by enamel loss or delamination near the dentin-enamel junction (DEJ), this study evaluated enamel and dentin nano-mechanical properties and chemical composition before and after simulated oral cancer radiotherapy.

**Design**—Sections from seven non-carious third molars were exposed to 2 Gy fractions, 5 days/week for 7 weeks for a total of 70 Gy. Nanoindentation was used to evaluate Young's modulus, while Raman microspectroscopy was used to measure protein/mineral ratios, carbonate/phosphate ratios, and phosphate peak width. All measures were completed prior to and following radiation at the same four buccal and lingual sites 500 and 30 microns from the DEJ in enamel and dentin (E-500, E-30, D-30 and D-500).

**Results**—The elastic modulus of enamel and dentin was significantly increased ( $P < 0.05$ ) following radiation. Based on Raman spectroscopic analysis, there was a significant decrease in the protein to mineral ratio (2931/430  $\text{cm}^{-1}$ ) following radiation at all sites tested except at D-500, while the carbonate to phosphate ratio (1070/960  $\text{cm}^{-1}$ ) increased at E-30 and decreased at D-500. Finally, phosphate peak width as measured by FWHM at 960  $\text{cm}^{-1}$  significantly decreased at both D-30 and D-500 following radiation.

**Conclusions**—Simulated radiotherapy produced an increase in the stiffness of enamel and dentin near the DEJ. Increased stiffness is speculated to be the result of the radiation-induced decrease in the protein content, with the percent reduction much greater in the enamel sites. Such changes in mechanical properties and chemical composition could potentially contribute to DEJ biomechanical failure leading to enamel delamination that occurs post-radiotherapy. However,

---

© 2015 Published by Elsevier Ltd.

Corresponding Authors: Dr. Mary P. Walker\* and Dr. Yong Wang, Department of Oral and Craniofacial Sciences, Center of Excellence in Musculoskeletal and Dental Tissues, University of Missouri-Kansas City School of Dentistry, 650 East 25<sup>th</sup> St, Kansas City, MO 64108, walkemp@umkc.edu; wangyo@umkc.edu, \*Phone: +1-816-235-2825, Fax: +1-816-235-5524.

**Publisher's Disclaimer:** This is a PDF file of an unedited manuscript that has been accepted for publication. As a service to our customers we are providing this early version of the manuscript. The manuscript will undergo copyediting, typesetting, and review of the resulting proof before it is published in its final citable form. Please note that during the production process errors may be discovered which could affect the content, and all legal disclaimers that apply to the journal pertain.

other analyses are required for a better understanding of radiotherapy-induced effects on tooth structure to improve preventive and restorative treatments for oral cancer patients.

### Keywords

Raman microspectroscopy; nanoindentation; radiotherapy; oral cancer; enamel; dentin-enamel junction; dentin

---

### Introduction

Radiotherapy is routinely prescribed to treat patients diagnosed with oral cancer. However, multiple radiation-induced complications occur after radiotherapy treatment such as mucositis, taste loss, xerostomia, and severe dentition breakdown that can result in loss of masticatory function.<sup>1–5</sup> Radiation-induced dentition breakdown begins to occur within the first year following radiotherapy and over time becomes more severe.<sup>1</sup> Post-radiation lesions differ in location and pattern of development and progression as compared to caries in non-radiated patients. For example, instead of pits, fissures and inter-proximal sites, post-radiation dental lesions develop at cervical, cuspal, and incisal areas, sites exposed to occlusal loading and associated flexure and considered more resistant to dental decay. Additionally, post-radiation lesions develop with initial enamel loss that can potentially result in partial to total enamel delamination leaving the exposed dentin vulnerable to subsequent decay.<sup>6, 7</sup>

Various factors likely contribute to post-radiation dentition breakdown but it has previously been thought to be an indirect effect due to irradiation-induced changes in salivary gland tissue resulting in hyposalivation.<sup>1, 2, 5</sup> However, we completed a clinical study and reported that the severity of dentition breakdown is also linked to the individual tooth dose with three tiers of tooth dose-response.<sup>8</sup> Minimal tooth damage occurs below 30 Gy; there is a 2–3x increased risk of tooth breakdown between 30–60 Gy likely related to salivary gland impact; and a 10x increased risk of tooth damage when the tooth-level dose is >60 Gy indicating radiation-induced damage to the tooth in addition to salivary gland damage. These findings suggest a direct effect of radiation on tooth structure with increasing radiation dose to the tooth.

To better understand radiotherapy-induced dentition breakdown distinguished by biomechanical failure of the dentin-enamel junction (DEJ) leading to enamel delamination, our group is focused on characterizing the structure, properties, and composition of enamel and dentin associated with the DEJ as well as post-radiation changes to those tissues. We recently demonstrated a protein-based enamel matrix layer containing type VII and type IV collagen that bridges with the DEJ in adult teeth.<sup>9–11</sup> This organic matrix layer is distributed along the enamel inner region, appears proportional in thickness to the anatomical enamel layer, and may play a role in stabilization of the DEJ. Next steps are to evaluate any radiation-induced changes that might occur within the enamel and dentin associated with the DEJ. While there have been previous evaluations of mechanical properties of enamel and dentin following *in vitro* radiation, the results are not consistent. Some studies reported changes in dentin and enamel of extracted tooth specimens radiated with doses greater than

60 Gy.<sup>12–15</sup> Another recent study reported mechanical property changes in enamel at lower *in vitro* doses (10–30 Gy) but no significant change at higher doses (40–60 Gy), while dentin mechanical property changes occurred at doses ranging from 10–60 Gy.<sup>16</sup> Conversely, other studies stated there was no significant change in mechanical properties<sup>17</sup> or chemical composition<sup>18</sup> of enamel and dentin following radiation to sterilize extracted teeth. Nevertheless, there is great variability within the experimental methods of these various studies including differences in storage time and storage solution of the tooth specimens that could affect results<sup>19–21</sup> as well differences as to how and where the tooth properties were measured, another factor that could affect results.<sup>22–24</sup> Finally, another important source of variability is the differences between teeth between patients and even within the same patient.<sup>25–27</sup>

Although previous studies correlated chemical structure with mechanical properties of non-radiated teeth<sup>28–30</sup>, similar studies have not been done to evaluate the effects of radiotherapy on tooth structure. With the combined use of nanoindentation and Raman microspectroscopy, we proposed to measure nano-mechanical properties and chemical composition of teeth from similar positions on the same tooth before and after radiation simulating oral cancer radiotherapy.

## Materials and Methods

Seven non-carious third molars previously extracted from individuals aged 18–20 years old were collected according to a protocol approved by the University of Missouri-Kansas City adult health science institutional review board. Excess soft tissue was removed and the teeth were stored at 4°C in phosphate buffered saline (PBS, pH 7.4) with 0.002% sodium azide as a microbial inhibitor. A slow-speed water-cooled diamond saw (Buehler Ltd, Lake Bluff, IL, USA), was used to remove the roots from the molars. The remaining crowns were then sectioned buccolingually to generate a 2-mm-thick cross-sectional slice centered on the mesiobuccal and mesiolingual cusps. After initial nanoindentation testing and Raman microspectroscopy, the sections were adhered in an upright position to a small glass cover slip (Thermo Scientific, Portsmouth, NH, USA) using sticky wax (Hygenic Corporation, Akron, OH, USA). Individual tooth sections were placed into a 20 ml scintillation vial (MidSci, St. Louis, MO, USA). Teeth sections were irradiated in a Varian 2100iX linear accelerator using an energy of 6 MV photons (Kansas City Cancer Centers, Kansas City, KS). To simulate oral cancer radiotherapy, teeth sections were exposed to 2 Gy fractions, five days a week for seven weeks for a total of 35 fractions equal to 70 Gy (frequent oral cancer dose). Additionally, to simulate reduced intraoral moisture conditions experienced by patients, enough PBS was placed in the vial to cover the slide but not submerge the tooth section. Following radiation, teeth sections remained in the vials with the same minimal amount of PBS and were stored at 4°C.

## Nanoindentation

Nanoindentation analyses were completed before and following radiation. Prior to analyses, the sections were sequentially polished under water using 600- and 1200-grit SiC paper and a ChemoMet polishing cloth (Buehler Ltd). For both pre- and post-radiation analyses, tooth

sections were evaluated at four buccal and lingual sites on a line located directly adjacent to the lowest portion of the occlusal fossa DEJ and parallel to the occlusal cusps. The sites were positioned 30  $\mu\text{m}$  and 500  $\mu\text{m}$  away from the DEJ in both enamel and dentin, E-500, E-30, D-30, D-500 (Fig. 1). At each site, five nanoindentations were done perpendicular to the line traversing the buccal and lingual sites with 5  $\mu\text{m}$  between indents.

Data points were acquired using a nanoindenter (Triboscope, Hysitron Inc., Minneapolis, MN, USA) attached to a Nanoscope IIIa atomic force microscope (Digital Instruments Inc., Santa Barbara, CA, USA). A diamond-tipped indenter with an equilateral triangular base (Berkovich geometry) was calibrated before mechanical data collection. Loading and unloading rates of 250  $\mu\text{N/s}$ , a holding segment time of 3 seconds, and a peak force of 2500  $\mu\text{N}$  were utilized. In order to prevent specimen drying, mechanical data was collected with the tooth section covered in distilled water.

Using the Oliver-Pharr method<sup>31</sup>, initial parts of the unloading curve obtained from generated force-displacement curves were analyzed to provide elastic modulus ( $E$ ) values for each nanoindentation. The values of Young's modulus of enamel and dentin were obtained via the Hysitron software based on the following equation:

Young's modulus:

$$\frac{1}{E_r} = \frac{1-v_m^2}{E_m} + \frac{1-v_i^2}{E_i}$$

Where  $v_m$  and  $E_m$  are Poisson's ratio and the elastic modulus of the material, respectively. In addition,  $v_i$  and  $E_i$  are Poisson's ratio and elastic modulus, respectively, for the indenter.

### Raman microspectroscopy

A LabRam HR 800 Raman spectrometer (Horiba Jobin Yvon, Edison, NJ, USA) operating at an excitation power of 20 mW with monochromatic radiation emitted by a He-Ne laser (632.8 nm) was used. During Raman data collection, the following parameters were used: 600 groove/mm grating, 400- $\mu\text{m}$  confocal hole, and 150- $\mu\text{m}$  slit width. Spectra were Raman-shift-frequency-calibrated using known lines of silicon.

Using the same approach as with nanoindentation, five Raman spectra were collected at each of the four buccal and lingual sites. Micro-Raman spectra were collected using a 100X-immersion objective (Olympus, 1.00w) focused on the tooth sections. Spectra were collected in the region of 50 to 4000  $\text{cm}^{-1}$  at 5- $\mu\text{m}$  intervals using a 60-s integration time for dentin and a 30-s integration time for enamel. A high-resolution monitor enabled visual identification of the position at which the Raman spectra were obtained.

### Spectral data analysis

Labspec 5 software (Horiba Jobin Yvon) was used to analyze the acquired Raman data. After spectral smoothing, the spectra were adjusted by manual multiple point baseline correction. The peak 2931  $\text{cm}^{-1}$  is assigned to the C-H stretching/deformation of organic matrix, the peak 430  $\text{cm}^{-1}$  is assigned to  $\nu_2$  vibration of the phosphate group in

hydroxyapatite. The  $\nu_2$  vibration peak of phosphate at  $430\text{ cm}^{-1}$  was selected as the internal standard for the normalization adjustment for the protein to mineral ratios.

The peak at  $1070\text{ cm}^{-1}$  is assigned to  $\nu_1$  vibration of the carbonate group (B type of carbonate) in hydroxyapatite; the peak at  $960\text{ cm}^{-1}$  is assigned to  $\nu_1$  vibration of the phosphate group in hydroxyapatite. The  $\nu_1$  vibration peak of phosphate at  $960\text{ cm}^{-1}$  was selected as the internal standard for the normalization adjustment of the mineral ratios.

Based on the Raman spectral data, the ratio of protein at  $2931\text{ cm}^{-1}$  to phosphate at  $430\text{ cm}^{-1}$  was calculated by integrating the area under the peaks to analyze differences in protein composition in both enamel and dentin. Likewise, the ratio of carbonate at  $1070\text{ cm}^{-1}$  to phosphate at  $960\text{ cm}^{-1}$  was obtained by integrating the area under the peaks to analyze differences in mineral composition in both enamel and dentin. In addition, the width of the phosphate peak at  $960\text{ cm}^{-1}$ , as measured by full-width at half-maximum (FWHM), was calculated at each spectrum to reflect the degree of crystallinity within enamel and dentin.<sup>32-34</sup>

### Statistical analyses

Overall mean and standard deviation (SD) for Young's modulus,  $2931/430\text{ cm}^{-1}$  ratio,  $1070/960\text{ cm}^{-1}$  ratio, and FWHM for  $960\text{ cm}^{-1}$  were calculated based on ten evaluations per site (5 measures at each buccal and lingual site, E-500, E-30, D-30, D-500) for each tooth section ( $n=7$ ). Because all evaluations were made before and after irradiation at the same sites, the data was compared using a repeated measures analysis of variance (RMANOVA) with the probability level for statistical significance set at  $\alpha = 0.05$ . With any significant outcomes, observed power and effect size (based on partial eta squared values), which accounts for the percent of dependent variable change associated with the independent variable (radiation), were also reported. Effect size can be used as a standardized index that is independent of sample size to quantify the effect of radiation on the dependent variables.<sup>35, 36</sup> Effect sizes, as previously described<sup>36</sup>, range from small (0.1–0.3), medium (>0.3–0.5), large (>0.5).

## Results

### Nanoindentation

The mean Young's modulus values and SD at the four measurement sites, E-500, E-30, D-30, D-500 are shown in Fig. 2. The RMANOVA indicated that at each measurement site modulus values were significantly higher ( $P < 0.05$ ) after radiation treatment *in vitro* with an observed power of 1.0. Additionally, the respective concomitant effect size at all measurement sites was greater than 0.50 indicating that 50% of the modulus increase is associated with radiation.

### Raman Microspectroscopy

Representative Raman spectra for E-30 and D-30, before and after radiation are presented in Fig. 3, with no noticeable differences observed following *in vitro* radiation. The mean and SD of the ratios,  $2931/430\text{ cm}^{-1}$ ,  $1070/960\text{ cm}^{-1}$ , and the FWHM at  $960\text{ cm}^{-1}$  at the same

measurement sites used for nanoindentation are presented in Figs. 4, 5, and 6, respectively. Based on the RMANOVA, the protein to mineral ratio ( $2931/430\text{ cm}^{-1}$ ) showed a significant ( $P < 0.05$ ) decrease at E-500, E-30, and D-30 after radiation with an observed power of at least 0.96 and an effect size of 0.32, 0.35, and 0.17, respectively. The carbonate to phosphate ratio ( $1070/960\text{ cm}^{-1}$ ) showed a significant ( $P < 0.05$ ) increase at E-30 with an observed power of 0.99 and an effect size of 0.26 and a significant decrease at D-500 with an observed power of 0.99 and an effect size of 0.28. Phosphate peak width as measured by FWHM at  $960\text{ cm}^{-1}$  showed a significant ( $P < 0.05$ ) decrease at both D-30 and D-500 with an observed power of 1.0 and an effect size of 0.30 and 0.40, respectively.

## Discussion

Because there is no methodology to allow testing teeth prior to and after *in vivo* radiotherapy, an important aspect of this study was developing an *in vitro* model that controlled as many variables as possible while simulating oral cancer radiotherapy. Based on the results using that model, there was a significant increase in elastic modulus after simulated oral cancer radiotherapy at the evaluated sites in enamel and dentin near the DEJ. Using a repeated measures study design, measurements were made before and after irradiation at the same buccal and lingual sites. Because there were no differences in the radiation effect between the halves, the buccal and lingual values were combined for each site, which also increased the sample size. The current results are dissimilar to previous reports of a decrease in elastic modulus and hardness<sup>14, 15</sup> or no significant change in mechanical properties following *in vitro* radiation.<sup>17</sup> Varying experimental methods including differences in storage solution, how and where tooth properties were measured and variances between and within patients may have contributed to the contradictory observed results.

For example, earlier studies reported a dramatic decrease of approximately 80% in both modulus and hardness even with low energy X-ray irradiation (125 keV) after a dose of 2 Gy.<sup>14, 15</sup> These studies utilized a storage medium of 0.09% sodium chloride (NaCl), which is reported to significantly decrease modulus and hardness values in enamel just after 1 day, and after 30 days storage in NaCl there was a 47% reduction in both hardness and modulus in dentin.<sup>19, 21</sup> Storage solution may be in part why these studies demonstrated a dramatic decrease in both modulus and hardness. In contrast, another study using gamma radiation for tooth sterilization reported no change in modulus or hardness<sup>17</sup> when tooth specimens were stored in Hank's balanced salt solution, which does not significantly alter the hardness or elastic modulus of enamel or dentin.<sup>20, 21</sup>

Measurement sites within teeth were also not well controlled in previous studies. An earlier study utilized a  $2\text{ mm}^2$  region of interest in both enamel and dentin, but no measureable distance from a defined landmark was described.<sup>15</sup> A later study from the same group used a similar sized region of interest; however, the protocol specified only that the enamel measurement was located in the cuspal zone and the dentin region was measured near the DEJ.<sup>14</sup> Similarly, another study provided no precise measurement site, merely that buccal and lingual sides in both enamel and intertubular dentin were measured.<sup>17</sup> Nevertheless, no quantifiable distance from the DEJ or from the outer edge of the enamel was detailed in any



of these studies. It has previously been shown that modulus and hardness values of enamel and dentin are dependent on location within the tooth, with values increasing with distance from the DEJ.<sup>22, 23, 30, 37</sup> Due to the gradient like nature of enamel and dentin it is imperative that experimental measurements be a calculable distance from a defined landmark within the tooth. Variability can also be dependent on tooth type<sup>26</sup>; thus, it is important to test paired specimens and/or regions from the same tooth section to control variability. Moreover, patient age has been shown to affect the elastic modulus and hardness of enamel<sup>22</sup>, and there is a change of the chemical composition and microstructure of dentin with increasing age.<sup>25</sup> Therefore, it is vital to account for age and include similar aged teeth when conducting comparative studies measuring mechanical properties.

As already indicated, this study included an *in vitro* model simulating oral cancer radiotherapy that accounted for as many variables as possible. It has been previously reported that there is a reduction in salivary function within the first week of radiotherapy that persists throughout treatment.<sup>38–40</sup> Even after just one fraction of the radiation treatment course, reduction in salivary flow was noted.<sup>41</sup> Therefore, in order to mimic reduced intraoral moisture conditions experienced by patients, rather than submerging tooth specimens in PBS, a humid environment was created by including a small amount of storage medium. While drying can affect mechanical properties of tooth specimens<sup>31</sup>, it is important to note that the specimens in this study remained moist throughout storage and testing. Besides moisture level, PBS was used as the storage solution, which as already mentioned does not significantly affect mechanical properties.<sup>19, 21</sup> Although oral cancer patients are not typically 18–20 year olds, third molars from patients in that age range were used in order to control other potential confounding variables such as patient age and tooth type. While simulated radiotherapy was completed at room temperature, following radiotherapy, teeth were stored at 4°C to inhibit microbial contamination and stabilize specimens prior to analyses to optimize the evaluation of radiation-induced effects only. Although the use of tooth sections does not directly simulate radiation of teeth in patients, this approach allowed us to measure properties before and after radiation at the same quantifiable sites 30 µm and 500 µm away from the DEJ in both dentin and enamel. We chose these dentin and enamel sites, since they symmetrically span the DEJ where post-radiotherapy enamel delamination initiates.

A previous study reported that there was no change in the calcium/phosphorous ratios or crystallinity of enamel following *in vitro* radiation at therapeutic levels.<sup>42</sup> Other studies have also speculated that therapeutic radiation exposure does not have a direct effect on the inorganic composition of teeth and suggest that changes within the organic matrix lead to enamel alterations that occur post-radiotherapy.<sup>16, 43</sup> However, our study was the first to evaluate chemical composition and mechanical properties in order to potentially explain the mechanism responsible for enamel delamination that can occur following radiotherapy. Phosphate as measured by FWHM of the peak at 960 cm<sup>-1</sup> and carbonate/phosphate (1070/960 cm<sup>-1</sup>) ratio have been used to explain hydroxyapatite crystallinity associated with carbonate content and correlated to modulus properties of enamel.<sup>30, 32, 33</sup> For instance, a decrease in phosphate peak width and the carbonate/phosphate ratio have been noted to correlate with an approximate 20% increase in modulus from inner to outer enamel.<sup>30</sup> While there was a 25–30% increase in modulus in both enamel and dentin following radiation

treatment, the associated phosphate and carbonate chemical composition changes that might be expected with increased modulus were not detected in radiated enamel. In accordance with previous studies<sup>16, 42, 43</sup> suggesting no radiation-induced change in the inorganic composition of enamel, no significant difference was observed for the carbonate/phosphate ratio at the E-500 measurement site or for phosphate peak width at either enamel site following irradiation. However, E-30 demonstrated a significant increase in the carbonate/phosphate ratio following irradiation. Future studies are needed to determine the cause of the observed increase in the carbonate/phosphate ratio in enamel near the DEJ following simulated radiotherapy *in vitro*. In contrast, both dentin sites showed a decreasing trend in phosphate peak width and carbonate/phosphate ratio after radiation, but this observed trend was minimal and likely inconsequential.

As already mentioned, previous studies speculate that radiotherapy alters the organic matrix of enamel.<sup>16, 43</sup> In the current study, the protein/mineral ratio decreased following simulated radiotherapy at all enamel and dentin sites with those differences being significant at E-500, E-30, and D-30, which supports the assumption of organic compositional changes following radiation treatment. A radiation-dependent decrease in the protein content as implied from the protein/mineral ratio data could explain the corresponding increase in modulus. Likewise, an earlier study reported an increase in elastic modulus as a result of lower organic content in enamel.<sup>44</sup> Mechanistically, we speculate that reductions in the protein/mineral ratio could be due in part to collagen structural alterations in both enamel and dentin. It is well known that dentin is composed primarily of type I collagen.<sup>45</sup> In addition, we have recently shown that both type IV and type VII collagen, as well as matrix metalloproteinase-20 (MMP-20), are present within the inner enamel organic matrix layer located adjacent to the dentinal surface.<sup>10, 11, 46</sup> Importantly, we have shown recently that type IV collagen immunoreactivity within the enamel organic matrix was dramatically reduced following high dose *in vivo* radiotherapy.<sup>11</sup> Accordingly, we speculate that an *in vitro* radiotherapy-induced reduction in dentinal type I collagen and/or type IV and type VII collagen in enamel could be due to direct radiolysis or indirectly, due to radiation activation of an MMP-catalyzed degradation, since radiation has been shown to activate existing MMPs in other tissues.<sup>47-49</sup> Whether direct or indirect, the radiation-induced decrease in the protein/mineral ratio could lead to the concomitant modulus increase. However, it is noteworthy that the relative percent reduction of the protein/mineral ratio was much larger at sites within the enamel organic matrix (44–77%) as compared to dentin sites (4–6%). Assuming enamel organic matrix components play a role in linking enamel to dentin, any radiation-induced change in that collagenous structure could potentially impact the stability of the DEJ leading to enamel delamination which occurs following radiotherapy. While we did not evaluate collagen degradation post-radiotherapy, an earlier study<sup>50</sup> using an *in vitro* radiation dose of 60 Gy reported increased amounts of collagen fragments in the skin, bone, and periosteum of porcine jaws due to direct radiogenic destruction. Another *in vitro* study<sup>16</sup> reported that with increasing irradiation dose (30 versus 60 Gy) there were increasing post-radiation morphological changes in the interprismatic structure of enamel coinciding with the enamel organic matrix. In dentin, the same study reported fragmentation of collagen fibers accompanied by the presence of fissures and the obliteration of tubules. Future studies are necessary to determine the cause of the reduced protein/mineral ratio following



simulated radiotherapy in vitro in this study. Other techniques like X-ray diffraction, nuclear magnetic resonance spectroscopy, collagen cross-linking analyses, and protein-specific biochemical analyses such as Western blotting and in situ zymography may be needed to discern specific chemical or biological changes that could be mechanistically linked to the decreased protein/mineral ratio and associated increased modulus following radiation.

In addition to our in vitro simulated radiotherapy analyses, preliminary analyses of in vivo radiated teeth from patients who have undergone radiotherapy to treat oral cancer have been initiated. Thus far, our preliminary in vivo data suggests similar mechanical property results to our in vitro study, higher modulus values in enamel and dentin near the DEJ following radiotherapy. Such changes in mechanical properties may be linked to pathologic enamel loss that occurs post-radiotherapy. However, further studies are needed to verify these results and then model how the altered properties would affect the stress distribution of the enamel-dentin interface using finite element method.

Finally, while it is important to understand the underlying mechanism linked to dentition breakdown following radiotherapy, it has also been demonstrated that in vitro radiation contributes to a decrease in bond strength of resin-based composite to both enamel and dentin, negatively impacting successful restoration of radiation-damaged teeth.<sup>51</sup> Thus, it is vital to develop protocols to minimize or counteract radiotherapy-induced damage to dental hard tissues, such as the simulated mouthwash protocols using sodium fluoride or chlorhexidine that were reported to prevent in vitro radiation-induced property changes of enamel and dentin.<sup>52</sup>

## Acknowledgments

This work was supported by NIH/NIDCR R01 grant DE021462. The authors also want to acknowledge the assistance of Steven Howard, (Kansas City Cancer Centers; Kansas City, KS) for his assistance with simulated radiotherapy treatment of tooth specimens.

## Abbreviations

<b>DEJ</b>	dentin-enamel junction
<b>Gy</b>	gray
<b>E-500</b>	enamel 500 microns from the DEJ
<b>E-30</b>	enamel 30 microns from the DEJ
<b>D-30</b>	dentin 30 microns from the DEJ
<b>D-500</b>	dentin 500 microns from the DEJ
<b>FWHM</b>	full-width at half-maximum
<b>PBS</b>	phosphate buffered saline
<b>ANOVA</b>	analysis of variance
<b><math>\nu</math></b>	Poisson's ratio
<b><math>E</math></b>	elastic modulus

## References

1. Vissink A, Jansma J, Spijkervet FK, Burlage FR, Coppes RP. Oral sequelae of head and neck radiotherapy. *Crit Rev Oral Biol Med*. 2003; 14(3):199–212. [PubMed: 12799323]
2. Kielbassa AM, Hinkelbein W, Hellwig E, Meyer-Luckel H. Radiation-related damage to dentition. *Lancet Oncol*. 2006; 7(4):326–35. [PubMed: 16574548]
3. Karmiol M, Walsh RF. Dental caries after radiotherapy of the oral regions. *J Am Dent Assoc*. 1975; 91(4):838–45. [PubMed: 1057626]
4. Anneroth G, Holm LE, Karlsson G. The effect of radiation on teeth. A clinical, histologic and microradiographic study. *Int J Oral Surg*. 1985; 14(3):269–74. [PubMed: 3926671]
5. Silva AR, Alves FA, Antunes A, Goes MF, Lopes MA. Patterns of demineralization and dentin reactions in radiation-related caries. *Caries Res*. 2009; 43(1):43–9. [PubMed: 19151554]
6. Jongebloed WL, Gravenmade EJ, Retief DH. Radiation caries. A review and SEM study. *Am J Dent*. 1988; 1(4):139–46. [PubMed: 3073790]
7. Jansma J, Vissink A, Jongebloed WL, Retief DH, Johannes's-Gravenmade E. Natural and induced radiation caries: A SEM study. *Am J Dent*. 1993; 6(3):130–6. [PubMed: 8240774]
8. Walker MP, Wichman B, Cheng A-L, Coster J, Williams KB. Impact of radiotherapy dose on dentition breakdown in head and neck cancer patients. *Pract Radiat Oncol*. 2011; 1(3):142–8. [PubMed: 21857887]
9. Dusevich V, Xu C, Wang Y, Walker MP, Gorski JP. Identification of a protein-containing enamel matrix layer which bridges with the dentine–enamel junction of adult human teeth. *Arch Oral Biol*. 2012; 57(12):1585–94. [PubMed: 22609172]
10. McGuire JD, Walker MP, Mousa A, Wang Y, Gorski JP. Type VII collagen is enriched in the enamel organic matrix associated with the dentin–enamel junction of mature human teeth. *Bone*. 2014; 63(0):29–35. [PubMed: 24594343]
11. McGuire JD, Gorski JP, Dusevich V, Wang Y, Walker MP. Type IV collagen is a novel DEJ biomarker that is reduced by radiotherapy. *J Dent Res*. 2014; 93(10):1028–34. [PubMed: 25146181]
12. Pioch T, Golfels D, Staehle HJ. An experimental study of the stability of irradiated teeth in the region of the dentinoenamel junction. *Endod Dent Traumatol*. 1992; 8(6):241–4. [PubMed: 1302687]
13. Soares CJ, Castro CG, Neiva NA, Soares PV, Santos-Filho PC, Naves LZ, et al. Effect of Gamma Irradiation on Ultimate Tensile Strength of Enamel and Dentin. *J Dent Res*. 2010; 89(2):159–64. [PubMed: 20042736]
14. Franzel W, Gerlach R. The irradiation action on human dental tissue by X-rays and electrons--a nanoindenter study. *Zeitschrift fur medizinische Physik*. 2009; 19(1):5–10. [PubMed: 19459580]
15. Franzel W, Gerlach R, Hein HJ, Schaller HG. Effect of tumor therapeutic irradiation on the mechanical properties of teeth tissue. *Zeitschrift fur medizinische Physik*. 2006; 16(2):148–54. [PubMed: 16875028]
16. Goncalves LM, Palma-Dibb RG, Paula-Silva FW, Oliveira HF, Nelson-Filho P, Silva LA, et al. Radiation therapy alters microhardness and microstructure of enamel and dentin of permanent human teeth. *J Dent*. 2014; 42(8):986–92. [PubMed: 24887361]
17. Brauer DS, Saeki K, Hilton JF, Marshall GW, Marshall SJ. Effect of sterilization by gamma radiation on nano-mechanical properties of teeth. *Dent Mater*. 2008; 24(8):1137–40. [PubMed: 18436298]
18. White JM, Goodis HE, Marshall SJ, Marshall GW. Sterilization of teeth by gamma radiation. *J Dent Res*. 1994; 73(9):1560–7. [PubMed: 7929992]
19. Anjum A, Otsuki M, Matin K, Tagami J. Preservation in the liquid media produces alterations in enamel surface properties. *J Dent*. 2009; 37(11):884–90. [PubMed: 19665832]
20. Habelitz S, Marshall GW Jr, Balooch M, Marshall SJ. Nanoindentation and storage of teeth. *J Biomech*. 2002; 35(7):995–8. [PubMed: 12052404]
21. Sultana S, Nikaido T, Asafujjoha M, Tagami J, Matin K. Storage media to preserve dentin and their effects on surface properties. *Int Chin J Dent*. 2006; 6:123–9.

22. Park S, Wang DH, Zhang D, Romberg E, Arola D. Mechanical properties of human enamel as a function of age and location in the tooth. *Journal of materials science*. 2008; 19(6):2317–24. [PubMed: 18157510]
23. Cuy JL, Mann AB, Livi KJ, Teaford MF, Weihs TP. Nanoindentation mapping of the mechanical properties of human molar tooth enamel. *Arch Oral Biol*. 2002; 47(4):281–91. [PubMed: 11922871]
24. Brauer DS, Hilton JF, Marshall GW, Marshall SJ. Nano- and micromechanical properties of dentine: Investigation of differences with tooth side. *J Biomech*. 2011; 44(8):1626–9. [PubMed: 21440894]
25. Duke ES, Lindemuth J. Variability of clinical dentin substrates. *Am J Dent*. 1991; 4(5):241–6. [PubMed: 1810335]
26. Hobson RS, McCabe JF, Hogg SD. Bond strength to surface enamel for different tooth types. *Dent Mater*. 2001; 17(2):184–9. [PubMed: 11163390]
27. Whittaker D. Structural variations in the surface zone of human tooth enamel observed by scanning electron microscopy. *Arch Oral Biol*. 1982; 27(5):383–92. [PubMed: 6956250]
28. Zheng Q, Xu H, Song F, Zhang L, Zhou X, Shao Y, et al. Spatial distribution of the human enamel fracture toughness with aging. *J Mech Behav Biomed Mater*. 2013; 26(0):148–54. [PubMed: 23768625]
29. Gallagher RR, Balooch M, Balooch G, Wilson RS, Marshall SJ, Marshall GW. Coupled Nanomechanical and Raman Microspectroscopic Investigation of Human Third Molar DEJ. *J Dent Biomech*. 2010; 1:1–8.
30. Xu C, Reed R, Gorski J, Wang Y, Walker M. The distribution of carbonate in enamel and its correlation with structure and mechanical properties. *Journal of materials science*. 2012; 47(23): 8035–43. [PubMed: 25221352]
31. Lewis G, Nyman JS. The use of nanoindentation for characterizing the properties of mineralized hard tissues: State-of-the art review. *J Biomed Mater Res Part B: Appl Biomater*. 2008; 87B(1):286–301.
32. Freeman JJ, Wopenka B, Silva MJ, Pasteris JD. Raman Spectroscopic Detection of Changes in Bioapatite in Mouse Femora as a Function of Age and In Vitro Fluoride Treatment. *Calcif Tissue Int*. 2001; 68(3):156–62. [PubMed: 11351499]
33. Pucéat E, Reynard B, Lécuyer C. Can crystallinity be used to determine the degree of chemical alteration of biogenic apatites? *Chem Geol*. 2004; 205(1–2):83–97.
34. Parayanthal P, Pollak FH. Raman Scattering in Alloy Semiconductors: “Spatial Correlation” Model. *Phys Rev Lett*. 1984; 52(20):1822–5.
35. Coe, R. It’s the Effect Size, Stupid; What effect size is and why it is important. Annual Conference of the British Educational Research Association; England: University of Exeter; 2002.
36. Cohen, J. *Statistical Power Analysis for the Behavioral Sciences*. 2. Hillsdale, NJ: Lawrence Erlbaum Associates, Inc; 1988. p. 280-7.
37. Meredith N, Sherriff M, Setchell DJ, Swanson SA. Measurement of the microhardness and Young’s modulus of human enamel and dentine using an indentation technique. *Arch Oral Biol*. 1996; 41(6):539–45. [PubMed: 8937644]
38. Deasy JO, Moiseenko V, Marks L, Chao KS, Nam J, Eisbruch A. Radiotherapy dose-volume effects on salivary gland function. *Int J Radiat Oncol Biol Phys*. 2010; 76(3 Suppl):S58–63. [PubMed: 20171519]
39. Dreizen S, Brown LR, Handler S, Levy BM. Radiation-induced xerostomia in cancer patients. Effect on salivary and serum electrolytes. *Cancer*. 1976; 38(1):273–8. [PubMed: 7352]
40. Marks JE, Davis CC, Gottsman VL, Purdy JE, Lee F. The effects of radiation of parotid salivary function. *Int J Radiat Oncol Biol Phys*. 1981; 7(8):1013–9. [PubMed: 7298398]
41. Leslie MD, Dische S. The early changes in salivary gland function during and after radiotherapy given for head and neck cancer. *Radiother Oncol*. 1994; 30(1):26–32. [PubMed: 8153377]
42. Zach GA. X-ray diffraction and calcium-phosphorous analysis of irradiated human teeth. *J Dent Res*. 1976; 55(5):907–9. [PubMed: 1067306]

43. Jansma J, Buskes JA, Vissink A, Mehta DM, Gravenmade EJ. The effect of X-ray irradiation on the demineralization of bovine dental enamel. A constant composition study. *Caries Res.* 1988; 22(4):199–203. [PubMed: 3165710]
44. He LH, Swain MV. Enamel--a functionally graded natural coating. *J Dent.* 2009; 37(8):596–603. [PubMed: 19406550]
45. Van Strijp AJ, Klont B, Ten Cate JM. Solubilization of dentin matrix collagen in situ. *J Dent Res.* 1992; 71(8):1498–502. [PubMed: 1506516]
46. McGuire JD, Mousa AA, Zhang BJ, Todoki LS, Huffman NT, Chandrababu KB, et al. Extracts of irradiated mature human tooth crowns contain MMP-20 protein and activity. *J Dent.* 2014; 42(5): 626–35. [PubMed: 24607847]
47. Strup-Perrot C, Vozenin-Brotans MC, Vandamme M, Benderitter M, Mathe D. Expression and activation of MMP -2, -3, -9, -14 are induced in rat colon after abdominal X-irradiation. *Scand J Gastroenterol.* 2006; 41(1):60–70. [PubMed: 16373278]
48. Araya J, Maruyama M, Sassa K, Fujita T, Hayashi R, Matsui S, et al. Ionizing radiation enhances matrix metalloproteinase-2 production in human lung epithelial cells. *Am J Physiol Lung Cell Mol Physiol.* 2001; 280(1):L30–8. [PubMed: 11133492]
49. Gogineni VR, Kargiotis O, Klopfenstein JD, Gujrati M, Dinh DH, Rao JS. RNAi-mediated downregulation of radiation-induced MMP-9 leads to apoptosis via activation of ERK and Akt in IOMM-Lee cells. *Int J Oncol.* 2009; 34(1):209–18. [PubMed: 19082492]
50. Açil Y, Springer I, Niehoff P, Gaßling V, Warnke P, Açmaz S, et al. Proof of Direct Radiogenic Destruction of Collagen in Vitro. *Strahlenther Onkol.* 2007; 183(7):374–9. [PubMed: 17609870]
51. Naves L, Novais V, Armstrong S, Correr-Sobrinho L, Soares C. Effect of gamma radiation on bonding to human enamel and dentin. *Support Care Cancer.* 2012; 20(11):2873–8. [PubMed: 22415607]
52. Soares CJ, Neiva NA, Soares PB, Dechichi P, Novais VR, Naves LZ, et al. Effects of chlorhexidine and fluoride on irradiated enamel and dentin. *J Dent Res.* 2011; 90(5):659–64. [PubMed: 21335538]

- Research focused on oral cancer radiotherapy-induced dentition breakdown
- Enamel & dentin properties and composition before/after simulated radiotherapy
- Increased stiffness and decreased protein of enamel and dentin near the DEJ may contribute to DEJ failure post-radiotherapy

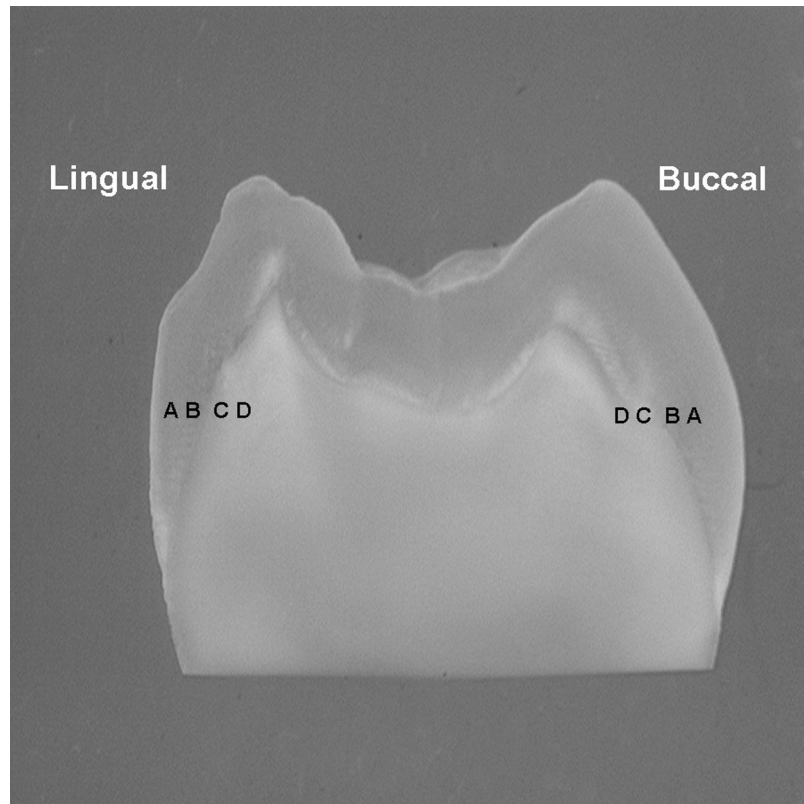


**Fig. 1.** Photograph of a tooth section showing the sites where mechanical property and chemical structure data were collected in relation to the buccal and lingual DEJ. Data was collected via 5 measures per site, with measurements done perpendicular to a line traversing the buccal and lingual sites with 5  $\mu\text{m}$  between measurement points; A = 500  $\mu\text{m}$  into enamel; B = 30  $\mu\text{m}$  into enamel; C = 30  $\mu\text{m}$  into dentin; D = 500  $\mu\text{m}$  into dentin.



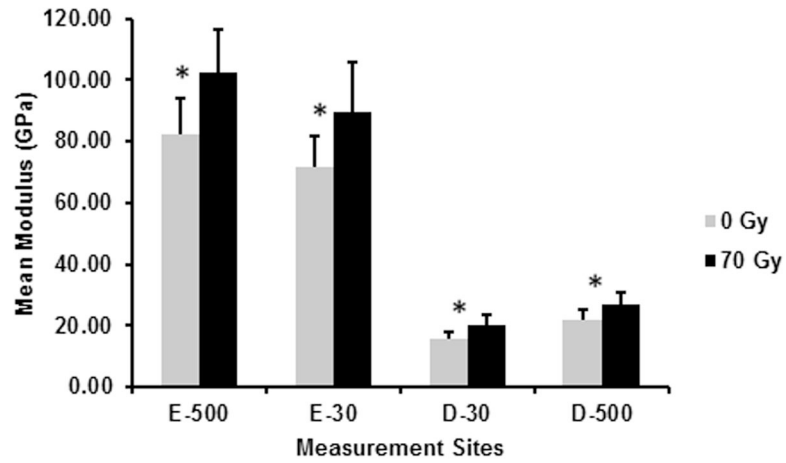


**Fig. 2.**

Mean modulus before (0 Gy) and after (70 Gy) simulated radiotherapy at eight sites related to the DEJ (4 buccal and 4 lingual sites; 5 measures/site/tooth; n=7 teeth): 500  $\mu$ m into enamel (E-500); 30  $\mu$ m into enamel (E-30); 30  $\mu$ m into dentin (D-30); 500  $\mu$ m into dentin (D-500). Error bars represent SD. \*Modulus was significantly higher (P 0.05) at all sites following simulated radiotherapy.

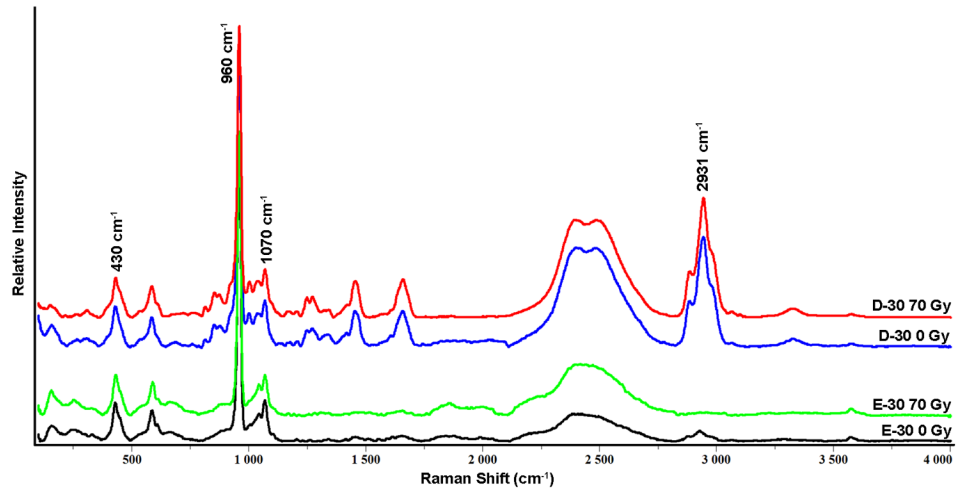


**Fig. 3.** Representative Raman spectra from enamel and dentin sites 30 microns from the DEJ (E-30 and D-30) from tooth sections before (0 Gy) and after (70 Gy) simulated radiotherapy. Spectra were normalized based on  $\nu_1$  of the phosphate  $960\text{ cm}^{-1}$  peak height.

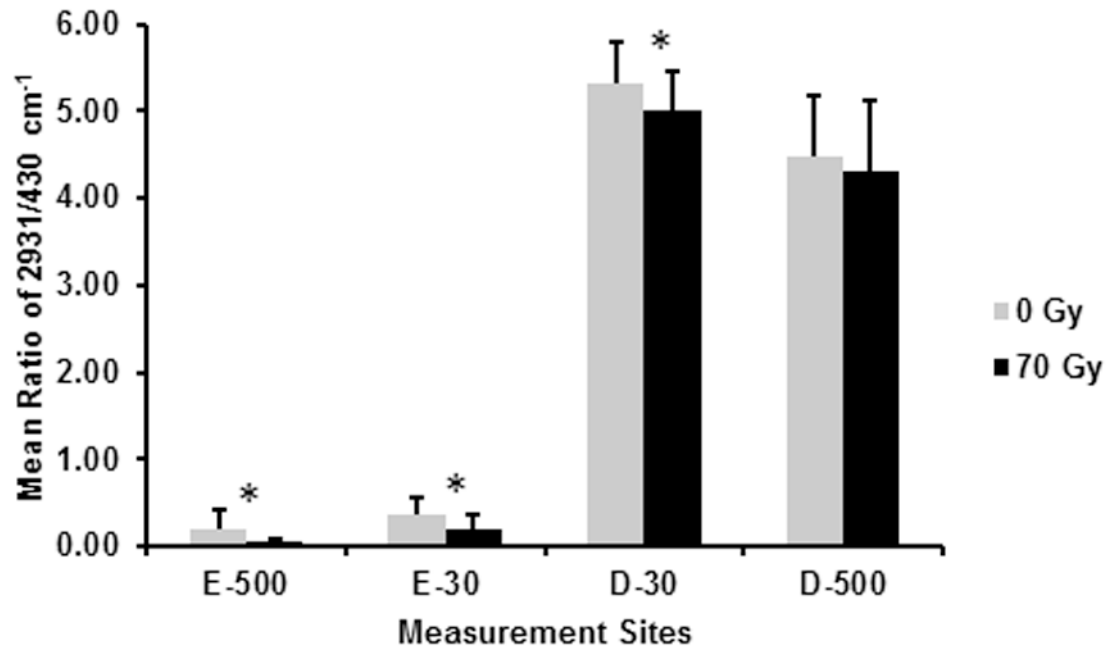


**Fig. 4.** Mean ratios of  $2931/430 \text{ cm}^{-1}$  (protein/mineral) before (0 Gy) and after (70 Gy) simulated radiotherapy at eight sites associated with the DEJ (4 buccal and 4 lingual sites; 5 spectra/site/tooth;  $n = 7$  teeth): 500  $\mu\text{m}$  into enamel (E-500); 30  $\mu\text{m}$  into enamel (E-30); 30  $\mu\text{m}$  into dentin (D-30); 500  $\mu\text{m}$  into dentin (D-500). Error bars represent SD. \*The protein/mineral ratio is significantly lower ( $P < 0.05$ ) at E-500, E-30, and D-30 following simulated radiotherapy.

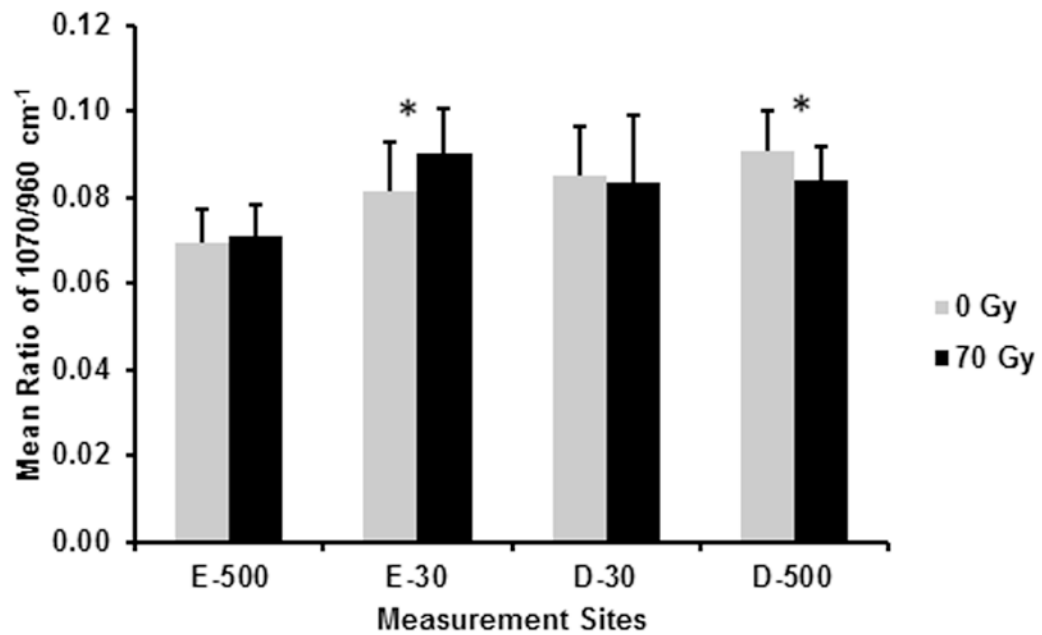


**Fig. 5.** Mean ratios of  $1070/960\text{ cm}^{-1}$  (carbonate/phosphate) before (0 Gy) and after (70 Gy) simulated radiotherapy at eight sites associated with the DEJ (4 buccal and 4 lingual sites; 5 spectra/site/tooth;  $n = 7$  teeth): 500  $\mu\text{m}$  into enamel (E-500); 30  $\mu\text{m}$  into enamel (E-30); 30  $\mu\text{m}$  into dentin (D-30); 500  $\mu\text{m}$  into dentin (D-500). Error bars represent SD. \*The carbonate/phosphate ratio is significantly higher ( $P < 0.05$ ) at E-30 and significantly lower at D-500 following simulated radiotherapy.

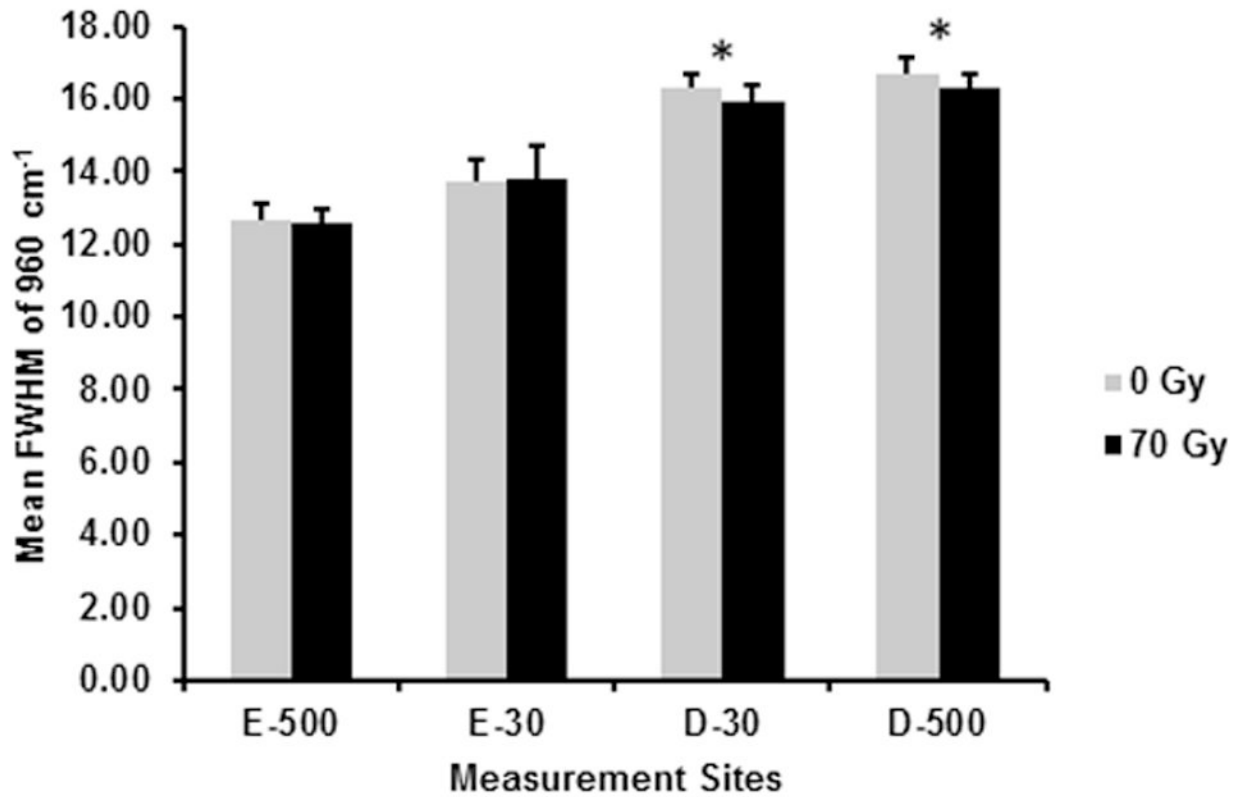


**Fig. 6.** Mean FWHM of  $960\text{ cm}^{-1}$  (phosphate peak width) before (0 Gy) and after (70 Gy) simulated radiotherapy at eight sites associated with the DEJ (4 buccal and 4 lingual sites; 5 spectra/site/tooth;  $n = 7$  teeth): 500  $\mu\text{m}$  into enamel (E-500); 30  $\mu\text{m}$  into enamel (E-30); 30  $\mu\text{m}$  into dentin (D-30); 500  $\mu\text{m}$  into dentin (D-500). Error bars represent SD. \*The peak width is significantly lower ( $P < 0.05$ ) at both dentin sites following simulated radiotherapy.